Guidelines for the design of (optimal) isothermal inactivation experiments

Peñalver-Soto, J. L., Garre, A., Esnoz, A., Fernández, P. S., & Egea, J. A.

Guidelines for the design of (optimal) isothermal inactivation experiments

Jose Lucas Peñalver-Soto[1], Alberto Garre[1,2*], Arturo Esnoz[1],Pablo S. Fernández[1], Jose A. Egea[3]

[1]Departamento de Ingeniería Agronómica, Instituto de Biotecnología Vegetal, Universidad Politécnica de Cartagena (ETSIA). Paseo Alfonso XIII, 48, 30203 Cartagena (Spain).

[2]Food Microbiology, Wageningen University & Research, P.O. Box 17, 6700 AA, Wageningen, the Netherlands

[3]Centro de Edafología y Biología Aplicada del Segura (CEBAS-CSIC), Campus Universitario de Espinardo, E-30100, Murcia, Spain

[*]corresponding author
alberto.garreperez@wur.nl

Abstract

Kinetic models are nowadays a basic tool to ensure food safety. Most models used in predictive microbiology have model parameters, whose precision is crucial to provide meaningful predictions. Kinetic parameters are usually estimated based on experimental data, where the experimental design can have a great impact on the precision of the estimates. In this sense, Optimal Experiment Design (OED) applies tools from optimization and information theory to identify the most informative experiment under a set of constrains (e.g. mathematical model, number of samples,etc). In this work, we develop a methodology for the design of optimal isothermal inactivation experiments. We consider the two dimensions of the design space (time and temperature), as well as a temperature-dependent maximum duration of the experiment. Functions for its application have been included in the *bioOED* R package.

We identify design patterns that remain optimum regardless of the number of sampling points for three inactivation models (Bigelow, Mafart and Peleg) and three model microorganisms (*Escherichia coli, Salmonella* Senftemberg and *Bacillus coagulans*). Samples at extreme temperatures and close to the maximum duration of the experiment are the most informative. Moreover, the Mafart and Peleg models require some samples at intermediate time points due to the non-linearity of the survivor curve. The impact of the reference temperature on the precision of the parameter estimates is also analysed. Based on numerical simulations we recommend fixing it to the mean of the maximum and minimum temperatures used for the experiments. The article ends with a discussion presenting guidelines for the design of isothermal inactivation experiments. They combine these optimum results based on information theory with several practical limitations related to isothermal inactivation experiments. The application of these guidelines would reduce the experimental burden required to characterize thermal inactivation.

Keywords: parameter estimation; predictive microbiology; pasteurization; microbial kinetics; robust statistics

1 Introduction

Predictive microbiology has become a basic tool for modern food science (McMeekin, Mellefont, & Ross, 2007). It develops mathematical models that can be applied to predict the microbial response (e.g. microbial growth or inactivation) for each step of the farm-to-fork chain that can be applied, for instance, in Quantitative Microbial Risk Assessment (Haas, Rose, & Gerba, 2014; Possas, Valdramidis, García-Gimeno, & Pérez-Rodríguez, 2019) or shelf-life estimation (García et al., 2015; González-Tejedor et al., 2017). Moreover, most model parameters have a biological meaning, which enables statistical inference to compare microbial responses. This allows, for instance, the identification of the most relevant sources of uncertainty and variability (den Besten, Wells-Bennik, &Zwietering, 2018) or the comparison between different treatments (Ros-Chumillas, Garre, Maté, Palop, &Periago, 2017).

Most mathematical models used in the context of predictive microbiology contain model parameters whose values are usually unknown and must be estimated based on experimental data. Due to experimental error (understood as the uncertainty and variability associated to data), exact values cannot be calculated for the model parameters (Box, Hunter, & Hunter, 2005). Instead, a measure of uncertainty must be reported associated to each model parameter (e.g. standard deviation). Reviews dealing with the parameter estimation problem (also called "inverse problem") in the context of food science can be found in the recent literature(Dolan & Mishra, 2013; Vilas, Arias-Mendez, Garcia, Alonso, & Balsa-Canto, 2018).

The uncertainty in parameter values is propagated when calculating predictions using mathematical models based on experimental data(Vilas et al., 2018).This uncertainty in the parameter estimates has a direct impact on risk management(Havelaar et al., 2010; Thompson, 2002; Garre, Boué, Fernández, Membré & Egea, 2019). A reduction in parameter uncertainty would also reduce the uncertainty of the predictions, providing decision makers with more accurate information relevant for risk assessment. The usual approach to reduce the uncertainty

of parameter estimates is an increase in the number of sampling points. However, this can be costly in the context of food science, due to the need of expensive equipment and highly trained personnel, among other factors. Optimal Experimental Design (OED) has the goal of identifying the most informative experimental designs given some constraints (e.g. mathematical model, number of sampling points, temperature range...). OED has been applied in a broad range of fields, enabling to estimate model parameters with higher accuracy than with "classical" (factorial/uniform) designs when the same number of data points is taken (Balsa-Canto, Alonso, &Banga, 2008; Balsa-Canto, Rodriguez-Fernandez, &Banga, 2007; Schenkendorf, Xie, Rehbein, Scholl, &Krewer, 2018).

In the context of microbial growth and inactivation, OED has been successfully applied in several cases, increasing the precision of parameter estimates with respect to uniform designs(Cunha, Oliveira, Brandão, & Oliveira, 1997; Frías, Oliveira, Cunha, & Oliveira, 1998; Garre, González-Tejedor, Peñalver-Soto, Fernández, &Egea, 2018; D.A. Longhi et al., 2017; Daniel Angelo Longhi et al., 2018; Paquet-Durand, Zettel, &Hitzmann, 2015; Stamati, Akkermans, Logist, Noriega, & Van Impe, 2016; van Derlinden, Balsa-Canto, & Van Impe, 2010). However, these studies were restricted to finding the most informative sampling times in one (dynamic or static) experiment. Currently, the most popular approach for this characterization is the application of several isothermal inactivation treatments at different temperatures. These data is, then, fitted using preferably a one-step algorithm (den Besten, Berendsen, Wells-Bennik, Straatsma, & Zwietering, 2017; Fernández, Ocio, Fernández, Rodrigo, & Martinez, 1999). Therefore, the design space is two-dimensional, with the sampling time and the treatment temperature as the design variables. To the knowledge of the authors, no methodology for OED has been developed in this context. This can be attributed to the fact that isothermal experiments, despite being simpler from an experimental point of view, are more complex from the point of view of experimental design. The design space in a set of

isothermal designs is two-dimensional design space, whereas the one in dynamic experiments is one-dimensional, increasing the complexity of the optimization problem required for OED. Furthermore, the maximum duration of an inactivation experiment is defined by the detection limit. In dynamic experiments, this restriction can easily be implemented, whereas in isothermal experiments the time required for the microbial count to reach the detection limit is a function of temperature. This defines a constraint that increases the complexity of the optimization problem.

In this work, a methodology based on the optimization of the Fisher Information Matrix (*FIM*) is developed for the OED of isothermal inactivation experiments. The methodology is able to handle the complexities inherent to isothermal experiments; i.e. the two-dimensional sample space and the temperature-dependent detection limit. It is applied for three different inactivation models commonly used in food science (Bigelow, Mafart and Peleg) and three different model microorganisms (*Escherichia coli, Salmonella* Senftemberg and *Bacillus coagulans*). Functions for applying this methodology have been included in the *bioOED* R package (Garre, Penalver, Fernandez, & Egea, 2017), making them available for the scientific community. This package is available on CRAN (https://CRAN.R-project.org/package=bioOED).

2. Materials and methods

2.1. Mathematical modelling of microbial inactivation

The OED has been calculated for three inactivation models commonly used in predictive microbiology: Bigelow(Bigelow, 1921), Mafart(Mafart, Couvert, Gaillard, &Leguerinel, 2002) and Peleg(Peleg& Cole, 1998). Note that, in order to ease the calculations for the OED, the initial microbial count is not considered as a parameter to estimate. Therefore, the decimal

logarithm of the fraction of survivors is the dependent variable, instead of the (log-)microbial count.

The Bigelow model considers a log-linear relationship between the fraction of survivors (S) and the elapsed time (t), as shown in Equation (1).

$$\log_{10} S = -\frac{1}{D(T)} t \quad (1)$$

The D-value at temperature$T$, $D(T)$, represents the time required to reduce the microbial population by 90% with a thermal treatment at temperature, *T*. This model also assumes a log-linear relationship between the D-value and temperature, as shown in Equation (2). This equation introduces the z-value (z) that quantifies the sensitivity of the D-value to temperature changes, indicating the temperature increase required for a ten-fold reduction of the D-value. The reference temperature, T_{ref}, has no biological meaning but can improve parameter identifiability(Poschet, Geeraerd, Van Loey, Hendrickx, & Van Impe, 2005).

$$log_{10}\, D(T) = \; log_{10} D_{ref} - \frac{T - T_{ref}}{z} \quad (2)$$

Both the Mafart and Peleg models belong to the family of weibullian models, which introduce a non-linearity in the isothermal survivor curve based on the hypothesis that the resistance of individual cells to the thermal stress follows a Weibull distribution. The Mafart model is expressed as shown in Equation (3), where $\delta(T)$, usually called the δ-value at temperature *T*, can be interpreted as the time required for the first log-reduction of the microbial density for a treatment at temperature *T*. The p value is the shape factor of the underlying Weibull distribution, which describes the concavity direction of the isothermal inactivation survivor curve. When the shape factor is larger than one, the curve has downwards concavity, whereas when it is lower than one there is a tail. If $p = 1$, the shape of the isothermal survivor curve is log-linear and the results are equivalent to those obtained using the Bigelow model for $D(T) = \delta(T)$.

$$log_{10}\, S = \, -\left(\frac{t}{\delta(T)}\right)^{p} \tag{3}$$

The Mafart model, similarly to the Bigelow model, hypothesizes that the inactivation rate follows an exponential relationship with temperature, using the secondary model shown in Equation (4). In this model, the z-value, z, and the reference temperature, T_{ref}, have the same interpretation as in the Bigelow model. The parameter δ_{ref} represents the value of $\delta(T)$ estimated at the reference temperature.

$$log_{10}\, \delta(T) = \, log_{10}\delta_{ref} - \frac{T - T_{ref}}{z} \tag{4}$$

The Peleg model uses a different parameterization of the primary model than the one used by Mafart, using$b(T)$instead of$\delta(T)$, as shown in Equation (5). Both parameters are related via the identity $b(T) = \left(1/\delta(T)\right)^{p}$. In addition, the shape factor is represented by n instead of *p*.

$$log_{10}\, S = \, -b(T) \cdot t^{n} \tag{5}$$

The Peleg model proposes a different secondary model than Bigelow or Mafart. It hypothesizes a log-logistic relationship between $b(T)$ and temperature, as shown in Equation (6). For temperatures much lower than the critical temperature (T_c), *b (T)* equals zero and no inactivation takes place. For values of temperature much higher than T_c, $b(T)$ has a linear relation with temperature with slope k. This model suggests a super-linear transition between both regimes.

$$b(T) = \ln\left(1 + e^{k(T - T_c)}\right) \tag{6}$$

In this study, we aim to define design patterns that are applicable to a broad range of microbial responses. Consequently, the microbial responses of three microorganisms with different inactivation kinetics have been extracted from the scientific literature: *Escherichia coli* in peptone water (Garre, Clemente-Carazo, Fernández, Lindqvist, &Egea, 2018), *Salmonella enteric* subsp. *enterica* serovar Senftenberg in peptone water (Huertas, Ros-

Chumillas, Esteban, Esnoz, &Palop, 2015) and *Bacillus coagulans* in nutrient broth supplemented with oregano oil (Haberbeck, Dannenhauer, Salomão, & De Aragão, 2013).These microorganisms present survivor curves with different shapes, that include upward and downward concavity, as well as linear responses. Furthermore, their D (and δ) valuesvariesby at least one order of magnitude. Table 1 summarizes the model parameters extracted and used as nominal parameters for the OED. This table also includes the parameters T_{max}andT_{min}, defining a theoretical, feasible temperature range for the isothermal inactivation experiments. The calculations have been repeated for different values of T_{max} and T_{min}, without any major impact on the conclusions of the study. Although the Bigelow model is not adequate to describe the microbial response of *S.* Senftemberg and *B. Coagulans* due to the non-linearity of the survivor curve, it has been included in the analysis to analyse how variations in the magnitude of the D and z-values affect the OED for this model.

2.2. A methodology for OED of isothermal inactivation experiments

We have applied for the OED of isothermal inactivation experiments an approach based on the optimization of the *FIM*. A complete description of the problem from a mathematical stand point can be found in the article by Asprey & Macchietto (2002). Isothermal inactivation experiments can be fitted using a "two-step" (model parameters are estimated sequentially) or a "one-step" (every model parameter is fitted in one step) approach. We have developed our methodology for the "one-step" fitting algorithm, which has proved more accurate than the "two-step" approach (den Besten et al., 2017; Fernández et al., 1999). Under the hypothesis of normality and homoscedasticity of the residuals, the *FIM* for an isothermal inactivation experiment with *n* sampling points can be calculated as shown in Equation (7).

$$FIM = \sum_{i=1}^{n} \left(\frac{\partial y}{\partial \theta}(t_i, T_i)\right)^T \cdot Q \cdot \left(\frac{\partial y}{\partial \theta}(t_i, T_i)\right) \tag{7}$$

The term$\partial y/\partial\theta_j(t_i,T_i)$representsthe local sensitivity functions, defined as the partial derivative of the response variable (the log-fraction of survivors in this study) with respect to the vector of model parameters,θ, evaluated at the sampling point defined by the vector (t_i,T_i).Q is a weight matrix, that will be considered as the identity matrix in this study. Because the local sensitivity functions are evaluated in the sampling points, the elements of the *FIM* depend on the experimental design; i.e. different combinations of time-temperature will result in different values of the *FIM* for the same model. This result is usually referred to as practical identifiability of the experimental design (Villaverde, 2019; Villaverde, Evans, Chappell, & Banga, 2019), which describes the ability to estimate the model parameters conditional to the design. It is, therefore, different to structural identifiability, which only depends on the mathematical model (Villaverde, Barreiro, & Papachristodoulou, 2016).

According to the Cramer-Rao inequality, the inverse of the *FIM* is a lower bound of the covariance matrix of the model parameters (*C*), which is closely related to the precision of the parameter estimates (i.e., smaller *C* implies less uncertainty). Therefore, experimental designs that maximize the *FIM* are likely to result in parameter estimates with lower uncertainty (Nishii, 1993). Because the *FIM* is a matrix, the optimization must be performed based on a metric. Several criteria are available in the literature, each one with a different interpretation (Balsa-Canto, Alonso, & Banga, 2008b). In this study, we have applied the D-criterion, that has already been successfully applied in similar problems (Garre, González-Tejedor, et al., 2018). This criterion consists on the maximization of the determinant of the *FIM*. Because of the Cramer-Rao inequality, the *FIM* can be used as an estimator of the variance-covariance matrix of the model parameters (de Aguiar, B. Bourguignon, Khots, Massart, &Phan-Than-Luu, 1995). Hence, an experimental design that maximizes the determinant of the *FIM* also minimizes the volume of the confidence ellipsoids of the model parameters. Therefore, it also minimizes the uncertainty associated to each model parameter (i.e. the size of the confidence intervals).

Therefore, the optimization problem required to calculate the optimal experiments can be written as shown in Equation (8), whereT_{min} and T_{max} define the suitable temperature range for the experiment andt_{max} is the maximum treatment time. Note that t_{max} is constant and does not consider the relationship between the time to reach the detectionlimit and the treatment temperature. In Section 2.2.2., a modification is included in the optimization problem to account for this relationship.

$$\max_{(t_i,T_i)} \det\left[\sum_{i=1}^{n}\left(\frac{\partial y}{\partial \theta}(t_i,T_i)\right)^{T}\cdot Q\cdot\left(\frac{\partial y}{\partial \theta}(t_i,T_i)\right)\right] \quad T_{min}\le T_i\le T_{max} \quad 0\le t_i\le t_{max} \tag{8}$$

2.2.1. Local sensitivity functions for isothermal inactivation

Local sensitivity functions are central for the OED methodology based on the optimization of the *FIM*. For isothermal conditions, the local sensitivity functions for the inactivation models considered in this study (Bigelow, Mafart and Peleg) have an analytical solution.

The Bigelow model has two model parameters (D_{ref} and z).The local sensitivity functions corresponding to them are shown, respectively, in Equations (9) and (10). Note that the reference temperature is not estimated using experimental data, so it is not considered a model parameter to fit.

$$\frac{\partial}{\partial\, D_{ref}}(\log S) = \frac{t\cdot 10^{\frac{T-T_{ref}}{z}}}{{D_{ref}}^2} \tag{9}$$

$$\frac{\partial}{\partial\, z}(\log S) = \frac{t\cdot \ln 10\,(T-T_{ref})\cdot 10^{-\frac{T-T_{ref}}{z}}}{{D_{ref}}^2} \tag{10}$$

The Mafart model has three model parameters (δ_{ref}, z and p). Their local sensitivity functions are reported in Equations (11), (12) and (13). As well as for the Bigelow model, the

local sensitivity functions of the reference temperature have not been calculated because it is not a parameter to fit.

$$\frac{\partial}{\partial\, \delta_{ref}}(\log S) = \frac{p \cdot t \cdot 10^{\frac{T-T_{ref}}{z}} \cdot \left(\frac{t \cdot 10^{\frac{T-T_{ref}}{z}}}{\delta_{ref}}\right)^{p-1}}{{\delta_{ref}}^2} \tag{11}$$

$$\frac{\partial}{\partial\, z}(\log S) = \frac{p \cdot t \cdot \ln 10\,(T - T_{ref}) \cdot 10^{\frac{T-T_{ref}}{z}} \cdot \left(\frac{t \cdot 10^{\frac{T-T_{ref}}{z}}}{\delta_{ref}}\right)^{p-1}}{\delta_{ref} \cdot z^2} \tag{12}$$

$$\frac{\partial}{\partial\, p}(\log S) = -\left(\frac{t \cdot 10^{\frac{T-T_{ref}}{z}}}{\delta_{ref}}\right)^{p} \log\left(\frac{t \cdot 10^{\frac{T-T_{ref}}{z}}}{\delta_{ref}}\right) \tag{13}$$

The Peleg model has three model parameters (k, n and T_c). The corresponding local sensitivity functions are written in Equations (14), (15) and (16).

$$\frac{\partial}{\partial\, k}(\log S) = \frac{(T_c - T) \cdot t^n \cdot e^{T \cdot k}}{e^{T_c \cdot k} + e^{T \cdot k}} \tag{14}$$

$$\frac{\partial}{\partial\, T_c}(\log S) = \frac{k \cdot e^{T \cdot k} \cdot t^n}{e^{T \cdot k} + e^{T_c \cdot k}} \tag{15}$$

$$\frac{\partial}{\partial\, n}(\log S) = -t^n \cdot \ln(t) \cdot \ln\left(e^{k(T-T_c)} + 1\right) \tag{16}$$

2.2.2. Consideration of a temperature-dependent detection limit in the OED

Inactivation experiments (in the absence of tail effects) reduce the microbial count until it is below the detection limit. Therefore, for time points after a maximum time, the microbial density is too low to provide any information. We refer to that maximum time in this article as *maximum treatment time* (t_{max}). Because the rate of inactivation grows with the treatment temperature, $t_{max}$is temperature-dependent. This introduces a constraint that must be included in the optimization problem (Equation 8), to avoid designs that cannot be carried out in the laboratory because they require a treatment duration larger than t_{max}.

Under the hypothesis that the inactivation model is correct, the treatment time (t_R) required to reach an arbitrary number of log-reductions (R) can be calculated from the primary and secondary models, as shown in equations (17), (18) and (19) for the Bigelow, Mafart and Peleg models, respectively. These formulas can predict the treatment time required to reach the detection limit at temperature T, i.e. $t_{max}(T)$.We have calculated the experimental designs for different values of the detection limit, without a major impact on the design patterns. Therefore, only the results calculated for an experiment duration corresponding to 6 log-reductions (equivalent to, e.g., an initial concentration of 7 log CFU/ml and a detection limit of 1 log CFU/ml) are reported in this article. Note that this number of log-reductions has not been selected based on any microbiological criteria, just as an illustration of the results. Nonetheless, the number of log-reductions does not affect optimal design patterns, so the results reported here are applicable for other conditions.

$$t_R = -R \cdot D_{ref} \cdot 10^{-\frac{T-T_{ref}}{z}} \tag{17}$$

$$t_R = -R^{1/p} \cdot \delta_{ref} \cdot 10^{-\frac{T-T_{ref}}{z}} \tag{18}$$

$$t_R = \left(-\frac{R}{\ln(1+e^{k(T-T_c)})}\right)^{1/n} \tag{19}$$

Equations (17), (18) or (19) have been added as a constraint to the optimization problem defined in Equation (8). Then, the optimal solution has been found applying the Enhanced Scatter Search algorithm (Egea, Martí, &Banga, 2010), using the implementation in the MEIGO R package (Egea et al., 2014). This algorithm is a heuristic optimization method based on evolutionary strategies. The constraint has been implemented through a mapping of the design space. If a point(t_i, T_i) is not feasible (i.e., $t_i > t_{max}(T_i)$) it is moved to $(t_{max}(T_i), T_i)$ to make it feasible. Therefore, the objective function outside the feasible area is "flat" in the time-coordinate.

2.3. Comparison of the accuracy of experimental designs using numerical simulations

The improved accuracy of the proposed designs with respect to "classical" uniform designs has been evaluated using *in-silico* experiments, according to the two methodologies proposed by Garre et al. (2019).The first one is based on the properties of the *FIM*. According to the Cramer-Rao inequality, the inverse of its determinant can be used as estimator of the volume of the confidence ellipsoids. The values of the determinant of the FIM can be plotted for different experimental designs to compare the amount of information that each one provides.

This approach, although computationally inexpensive, is only valid under several statistical hypotheses (e.g. linearity of the response, uncorrelated parameters) that are usually not fulfilled in microbial inactivation. Moreover, it is hard to estimate from the determinant of the *FIM* the precision (i.e. the standard error) of each model parameter. For that reason, Garre et al. (2019) also suggest a second approach that has less restrictive hypotheses than the *FIM* and provides more detailed information on the precision of parameter estimates, at the expense of computational cost. This second approach is based on Monte Carlo simulations of the observations that could be observed in a laboratory. The experimental error is modelled as a perturbation of the ideal response of the microorganism to the stress (the one obtained using the parameters in Table 1). In this work, a normal distribution with mean zero and $\sigma = 0.5$ has been used. This is repeated to simulate a large number of experiments (1000) and, then, the distributions of some index of the parameters. In this study, we have focused in their estimated values to analyse the bias and their standard errors for parameter precision. The simulations have been repeated for different values of σ, without observing any impact on the optimal design patterns. All the simulations and the model fits have been carried out using the functions included in the *bioinactivation* R package (Garre, Clemente-Carazo, et al., 2018; Garre, Fernández, Lindqvist, & Egea, 2017).

These numerical methods have been used to how the precision in parameter estimates varies as the number of sampling points is increased. Furthermore, they have been applied to compare between optimal and uniform experimental designs of different configurations. For isothermal inactivation experiments, due to the fact that the design space is two-dimensional, different uniform experiments can be calculated for the same number of data points. For each microorganism, uniform experiment designs with two (maximum and minimum), three (maximum, minimum and intermediate) and four (maximum, minimum and two intermediate) temperatures have been defined. For each temperature, the elapsed time has been divided uniformly in three to six sampling points. Figure 1 illustrates the three different types of uniform designs analysed.

3. Results

3.1. Local sensitivity functions for isothermal inactivation

Local sensitivities are a central part for the calculation of OEDs based on the *FIM*. Furthermore, they provide qualitative and quantitative information about the model analysed. Therefore, a sensitivity analysis has been carried out before calculating the OED. Figure 2illustrates the local sensitivity functions for the Bigelow, Mafart and Peleg models for each microorganism. The effect of the reference temperature on the sensitivity functions is illustrated in Supp. Figure 1. Because the design space is two-dimensional (time and temperature), each local sensitivity functions is a three-dimensional surface. Solid lines in Figure 2 and Supp. Figure 1 indicate combinations of treatment time and temperature with the same local sensitivity, whereas the background colour indicates the magnitude of the sensitivity function (i.e. the “height” of the surface).

The shape of the local sensitivities with respect to the three parameters of the Mafart model(Figure 2B, 2E and 2H) is affected by the characteristics of the microorganism and,

specially, by the reference temperature (supp. Figure 1). The slope of the surface calculated for *S.* Senftemberg is higher than for *B. coagulans*. The one for *E. coli* is in between both values. However, the topological shape of the surface is barely affected by the kinetic parameters of the microorganism. Modifications on the reference temperature, on the other hand, have a very relevant effect on the local sensitivities with respect to the z-value. Due to the secondary model used for the Mafart model (Equation 4), the local sensitivity with respect to this parameter for a temperature$T = T_{ref}$ equals zero. Therefore, fixing T_{ref} to different values shifts the location of this line with zero sensitivity. Furthermore, the shape of the local sensitivity function with respect to the z-value is not symmetrical with respect to the reference temperature. This can be visualized by comparing, for instance, Figure S1D and Figure S1F. Because of the crucial role of local sensitivities on the *FIM*, it is expected that changes in T_{ref} should modify the precision of the parameter estimates. This question is further analysed in section 3.2 of this article. Note that the local sensitivity functions for the Bigelow model are equivalent to those calculated for the Mafart model when $p = 1$ (D_{ref} equivalent to δ_{ref}). Hence, the observations made for the Mafart model can be extrapolated for the Bigelow model.

The local sensitivity of parameter *n* in the Peleg model is similar to the one of parameter *p* in the Mafart model. This was expected, because both parameters represent the shape factor of the underlying Weibull distribution used as hypothesis for the primary model. Local sensitivities with respect to k_b are similar in shape to those calculated for the z-value in the Mafart model. Both parameters are introduced in the secondary model to describe the relationship between the inactivation rate and changes in temperature (δ^{-1} is log-linear with slope z^{-1} in Mafart; b is linear with slope $k_b$in Peleg). Furthermore, the local sensitivity with respect to $k_b$equals zero when $T = T_{crit}$, similar to the relationship between z and T_{ref}. These similarities in the interpretation of both parameters result in similar sensitivity functions. Finally, the local sensitivities with respect to T_{crit} are similar to those with respect to δ_{ref}.

Because of these similarities, it is expected that both the Peleg and Mafart models, despite their different secondary models, have similar performance when describing isothermal microbial inactivation.

The methodology for OED based on the *FIM* tends to locate sampling points in areas of the design space (treatment time/temperature combinations) with high local sensitivity(Schenkendorf et al., 2018). According to Figure 2, the areas with the highest local sensitivity are located in the upper right corner of the design space, corresponding to high treatment times and temperatures. However, for microbial inactivation, the maximum treatment time is constrained by the time required to reach the detection limit, which is temperature dependent (dashed green line in these plots). Therefore, without a constraint to relate to the detection limit, we expect the OED to calculate designs that cannot be realized in the laboratory. This question is further analysed in section 3.3.

3.2. Impact of the reference temperature in the uncertainty of the parameter estimates

The reference temperature is a parameter without a biological interpretation that is included in the Bigelow and Mafart models to improve parameter identifiability (Dolan, Valdramidis, & Mishra, 2013a). As already discussed in the previous section, changes in the reference temperature affects the local sensitivity functions of the z-value. As described in the materials and methods section, we have simulated uniform designs with four temperatures and four samples per temperature tested for all microorganisms to analyse the impact of different values of the reference temperature in the precision of the parameter estimates. The precision in the z-value (in both models) and the p-value (in the Mafart one) was not affected by variations in the reference temperature. On the other hand, changes in the reference temperature affected the uncertainty associated to the D-value (Bigelow model) and δ-value (Mafart model). Figure 3 illustrates using boxplots the distribution of the relative standard deviation (estimated standard error divided by estimated value) of these parameters in 1000 simulated experiments

when the reference temperature is fixed to five different values (90ºC [T_{min}], 92.5ºC, 95ºC, 97.5ºC and 100ºC [T_{max}]).The reference temperature has a strong influence in the precision of the D-value of the Bigelow model (Figure 3A). Fixing it to an extreme value (T_{max} or T_{min}) results in the lowest precision, whereas setting it to the mean of the temperature range of the experiment(95ºC = (90 + 100)/2; in this case) results in a significant reduction in the expected relative standard deviation of this parameter. The expected relative standard deviation is reduced from 0.009 to 0.005. Figure 3A also shows that the effect of the reference temperature on the precision of the parameter estimates is symmetrical. The distribution of the relative standard deviation when the reference temperature equals the maximum temperature (100ºC) is indistinguishable from the one obtained for the minimum temperature (90ºC). This is also observed for other intermediate values, symmetrical with respect to the mean value (92.5 and 97.5ºC). This results are in-line with those obtained by Poschet et al. (2005).

The results obtained for the Mafart model (Figure 3B) are similar to those obtained for the Bigelow model. Again, the lowest uncertainty is obtained when the reference temperature is fixed to the mean of the maximum and minimum temperature. As well as for the Bigelow model, the effect of the reference temperature in the precision of the parameter estimates of the Mafart model is symmetrical; the same precision was obtained at 100 and 90ºC, and at 97.5 and 92.5ºC.However, the impact is much lower for the Mafart model than for the Bigelow model. The expected relative standard deviation is reduced from0.0253 to 0.0249 when the reference temperature is changed from 90º to 95ºC. This could be attributed to the correlation between the δ-value and parameter *p* of the Mafart model. However, an in-deep analysis of the structural and practical identifiability of the Mafart model would be required to confirm this hypothesis. That study has a high mathematical complexity (Villaverde, 2019; Villaverde et al., 2016) and is out of the scope of this article. The computational studied has also been carried out for other

designs (uniform and optimal), as well as for the other two microorganisms, obtaining qualitatively the same results (not reported).

Consequently, the selection of the reference temperature influences the uncertainty of the model parameters in the Bigelow and, to a lesser extent, the Mafart model. This implies thatthe uncertainty associated to the model parameters can be reduced by an adequate selection of the reference temperature, without the need of any additional experimental effort. According to the numerical results of this investigation, it is recommended to fix the reference temperature to the mean of the maximum and minimum temperatures used for the analysis. On a previous study Poschet et al. (2005) reached the same conclusion for isothermal inactivation when the two-step model fitting algorithm was used. Dolan, Valdramidis & Mishra (2013b), also applying Monte Carlo simulations, identified a reference temperature that minimized the correlation between the model parameters for several inactivation models. In the case of a model similar to the Bigelow model, they identified an optimum reference temperature close to the mean of the temperature range, as well as in our study. On the other hand, Datta(1993) proposes a formula to calculate a reference temperature that minimizes the error of the secondary model with respect to the Arrhenius equation. This procedure results in a reference temperature that is very close to the maximum temperature used in the experiments. The reason for this discrepancy is that the goal of the study by Datta was the minimization of the error in the model with respect to the Arrhenius model, not the optimization of the precision in the parameter estimates. The different target of his investigation is responsible for the differences in the result.

3.3. OED for isothermal inactivation

As a first step, OEDs have been calculated without considering the constraint regarding the detection limit (i.e. optimizing Equation 8). The optimal experiments calculated had most sampling points at the upper limits of the treatment time and temperature range (results not

shown). As already discussed, the OED based on the FIM tends to locate sampling points in areas with high local sensitivity. In the cases studied, the areas with the highest local sensitivity are located on the upper-right corner of the design space, as shown in Figure 2. Therefore, in the absence of a constraint, the optimal solution consists of sampling points in that area. However, these points are not feasible under actual laboratory conditions because the microbial count is well below the detection limit. These designs, despite optimal from the point of view of information theory, are not practical in actual laboratory conditions. Therefore, there is a need to include a constraint related to the detection limit.

OEDs have been calculated for every case studied (three models and three microorganisms) for a different number of sampling points (four to eighteen). The reference temperature has been set to the mean of the temperature range, according to the conclusions of section 3.2. Our results show that the optimal design pattern depends on the inactivation model selected, is slightly affected by the characteristics of the microorganism, and is not affected by the number of sampling points. The value of the reference temperature does not affect the optimal design patter (result not shown). As an illustration, the OEDs calculated for 10 sampling points are illustrated in Figure 2. For the Bigelow model, sampling points are located in two areas: at the values of $t_{max}(T)$ corresponding to T_{min} and T_{max}. That configuration would be unable to identify the value of p and n in the Mafart and Peleg models, respectively. Consequently, the OEDs calculated for both models include additional sampling points at intermediate treatment times. Nevertheless, the number of sampling points at intermediate treatment times is lower than those located for treatment times close to $t_{max}(T)$. For the Mafart model, sampling points are located in two additional locations with respect to the Bigelow model. These areas are also at the maximum and minimum temperature, but at an intermediate time instead of$t_{max}(T)$. The exact sampling time of these points depends on the value of the parameter p. For $p > 1$ (*B. coagulans*), the optimum configuration has points closer to t_{max}than

for $p < 1$ (*S.* Senftemberg), when the intermediate points are closer to the beginning of the treatment. Finally, for the Peleg model, one additional area is identified with respect to the Bigelow model. In this case, the additional sampling points are also located at an intermediate treatment time. Whereas in the Mafart model the additional points were located at T_{min} and T_{max}, the optimal design pattern in the Peleg model uses experiments at an intermediate temperature. The value of the couplet time-temperature of the additional sampling points depends on the characteristics of the microorganism. For $n > 1$ (*B. coagulans*), the optimum configuration is above the intermediate temperature and closer to the detection limit than when $n < 1$ (*S.* Senftemberg). In the latter case, the intermediate points are further from the detection limit and it has a temperature below the intermediate one. These optimum patterns were stable when the total number of sampling points was changed.

3.4. Comparison between optimal and uniform designs

In this section we compare the precision in parameter estimates that is attained with the proposed OEDs (considering the temperature-dependent restriction in the treatment time) with respect to uniform designs. Because the sampling space is two-dimensional (time and temperature), for a given number of sampling points, several uniform designs are possible. We have considered uniform designs with two different treatment temperatures ("Uni 2"), three temperatures ("Uni 3") and four temperatures ("Uni4"). In every design, the same number of samples has been used for each temperature. For instance, a "Uni 3" design with 12 sampling points has four samples atT_{max}, four at T_{min} and four at $T = (T_{max} + T_{min})/2$. Figure 1 shows an illustrative comparison of these designs.

Figure 4 plots the inverse of the determinant of the *FIM* calculated for experimental designs (uniform and optimal) for four to twenty sampling points. Note that, as justified in the materials and methods section, the inverse of the determinant of the *FIM* is an estimate of the volume of the confidence ellipsoids of the model parameters. In every case, an increase in the

455 number of sampling points reduces the uncertainty of the model parameters. The relationship
456 between the inverse of the determinant of the *FIM* and the number of sampling points is close
457 to log-linear. This implies that, when the number of samples is low, an increase in the number
458 of sampling points has a strong, positive influence in uncertainty. This impact, however, is
459 reduced as the number of samples is increased. This result is in agreement with those reported
460 by Garre et al. 2019 for dynamic inactivation experiments.

461 In every case studied, the OED provides parameter values with lower uncertainty than
462 uniform designs with a similar number of sampling points. Regarding the uniform designs, the
463 number of temperatures considered has a significant influence on the results. Designs with two
464 temperatures ("Uni 2") are more informative than those with three ("Uni 3"), which are more
465 informative than those with four temperatures ("Uni 4"). This can be explained based on the
466 patterns identified for optimal experiments in this context. For the Bigelow and the Mafart
467 model, the OED identifies sampling points at the maximum and minimum temperatures as the
468 most informative ones. A uniform experiment design with more than two different temperatures
469 places sampling points at intermediate temperatures, less informative than the extreme ones.
470 Consequently, because they are closer to the pattern defined by the optimal one, uniform
471 experiments with two temperatures are more informative than those with more temperatures for
472 the same number of sampling points.

473 Monte Carlo simulations have been used to further compare the precision and accuracy
474 of different experimental designs, extending the conclusions drawn from the observation of the
475 values of the FIM. An OED with12 sampling points has been compared against a uniform
476 designs with the same number of sampling points. Namely, we have considered uniform designs
477 with two different temperatures and six sampling points per temperature ("Uni_2_6"), three
478 different temperatures and four samples per temperature ("Uni_3_4"), and four different
479 temperatures and three samples per temperature ("Uni_4_3"). The comparison has been made

for the three microorganisms and three inactivation models studied in this investigation. For every experimental design and case studied, the mean of the parameter estimates matched the value used for the simulations, indicating a lack of bias. However, the precision varied between experimental designs. Figure5shows density plots of the relative standard deviations estimated in 1000 Monte Carlo simulations. For most cases, the OED systematically estimates parameters with a lower standard deviation than the uniform designs; i.e. with less uncertainty. This result is in line with the predictions made based on the values of the determinant of the *FIM*. The improvement is dependent on the mathematical model and the microorganism studied. For the Bigelow model, a 52% reduction in uncertainty for every microorganism and inactivation model is attained (for example with *B. coagulans* and Bigelow (Figure 5A) the expected relative standard deviation for D_{ref} is reduced from 0.011 to 0.007 and *z* is reduced from 0.015to 0.007). For the Mafart model, the improvement for the parameters δ_{ref} and p is only noticeable for the simulations on *S.* Senftemberg. This can be due to the high correlation between these two model parameters. Nevertheless, the OED significantly reduces the uncertainty of the estimate for the z-value in every case studied. For the Peleg model, the OED again results in a noticeable reduction in the uncertainty of every parameter estimate. The magnitude of this improvement, however, depends on the microorganism, being the improvement the biggest for the simulations in *S.* Senftemberg.

There are also differences between the precision attained for different uniform experimental designs. Uniform designs with two temperatures result in parameter estimates with lower standard deviations than designs with treatments at three or four different temperatures for every case studied. These results are in-line with the predictions made based on the determinant of the FIM. Again, they can be justified based on the fact that uniform designs with only two temperatures are more similar to the optimal design patterns.

4. Discussion

The importance of kinetic parameters for food science is hinted by the large number of scientific articles published during the last years dedicated to review them (Doyle & Mazzotta, 2000; Doyle, Mazzotta, Wang, Wiseman, & Scott, 2001). Although some studies have tried to provide tools to extrapolate the kinetic parameters already available in the literature (den Besten et al., 2018; van Asselt & Zwietering, 2006), in most cases, experimental data is required to estimate their values. Considering that inactivation experiments require specific equipment and media, as well as highly trained personnel, describing the microbial inactivation kinetics is a costly process. OED has the potential to reduce the experimental work (and the associated economic cost) required for this task. However, its application to food science remains mostly theoretical. Most applied studies use uniform designs or "optimal" designs based on heuristics and personal experience, rather than on a proper mathematical analysis. This can be attributed to the complexities associated to the calculation of an optimal design, which requires advanced concepts of statistics, numerical optimization and information theory. Moreover, experimental designs that may be optimal from the point of view of information theory may not be feasible from an experimental point of view, despite including some constraints in the optimization (e.g. the detection limit).

The results of this investigation enable the definition of several guidelines that would result in isothermal inactivation experiments that are optimal (or near optimal). Designs adhering to these guidelines are likely to results in more precise parameter estimates than uniform designs and designs based on experience. These guidelines combine the results obtained in this investigation based on information theory with several practical limitations related to experimental settings for inactivation experiments:

1. The use of an appropriate reference temperature can reduce the uncertainty associated to the parameter estimates. This is especially interesting, because it does

not require any modification in already existing laboratory protocols. According to the results of this investigation, it is recommended to set the reference temperature to the mean of the temperature range used for the experiments.

2. Data points taken at the minimum and maximum treatment temperatures are the most informative ones. Therefore, experimental efforts shall concentrate at these temperature treatments. Nonetheless, this result is valid as long as the mathematical models are valid. It is encouraged the performance of, at least, one repetition at an intermediate temperature to validate the assumptions of the secondary model (e.g. the log-linearity between the D-value and temperature).
3. For every model tested, the most informative points correspond to treatments time close to the one where the detection limit is reached. Taking samples close to the detection limit can be challenging in laboratory conditions, because the actual microbial kinetics are unknown. We recommend researchers to design experiments focusing experimental efforts at treatment times close to the maximum treatment time based, for instance, on kinetic data already available in the literature. Then, the experimental design can be updated after the first repetitions of the experiment. Note that sample times taken at sub-optimal treatment times, although less informative, will certainly reduce parameter uncertainty and will contribute to the validation of the hypotheses of the primary model. Therefore, the initial, suboptimal repetitions of the experiments are not a waste of resources.
4. The selection of the mathematical model more suitable to describe microbial inactivation remains an open research question in predictive microbiology. Based on the results of this investigation, we discourage to design experiments starting with the hypothesis that inactivation is log-linear. The OED for this mathematical model does not include samples at intermediate treatment times, so deviations from

log-linearity would pass unnoticed. Consequently, the Peleg or Mafart model should be used as starting hypothesis. Both models include a parameter to describe the curvature of the survivor curve, so a statistical test can be performed after model fitting to assess the significance of the non-linearities of the survivor curve.

5. The OEDs calculated in this study have identified few areas where data points should be collected (two for Bigelow, four for Mafart and three for Peleg). However, this does not imply that one sample taken in each one of those areas should suffice for model fitting. The characterization of the microbial response is subject to experimental error, so the parameter estimates are always affected by uncertainty(Chik, Schmidt, & Emelko, 2018; EFSA Scientific Committee et al., 2018; Garcés-Vega & Marks, 2014; Garre, Egea, Esnoz, Palop, & Fernandez, 2019; Jarvis, 2008). As a lower threshold, experiments shall be designed with a sufficient number of data points to consider the uncertainty in the parameter estimates and the predictions (e.g. an estimate of the standard deviation).

5. Conclusions

A methodology for the calculation of optimal experiments for isothermal inactivation has been developed. This methodology, based on the optimization of the FIM, is able to consider a two-dimensional design space (time and temperature), as well as a temperature-dependent detection limit. It has been applied to identify design patterns that are optimal from the point of view of information theory. These patterns are stable with respect to the number of sampling points. Furthermore, the effect of the reference temperature has been studied, concluding that the average of the temperature range tested is optimum from the point of view of the precision of parameter estimates. Numerical simulations have demonstrated that the proposed experimental designs are significantly more informative than uniform designs with the same number of sampling points. Based on these results, we define guidelines for the design

of isothermal inactivation experiments that combine these optimal results with several known experimental limitations. Their application would enable a reduction of the experimental work required to characterize the microbial response to static stresses.

Acknowledgments

The financial support of this research work was provided by the Ministry of Science, Innovation and Universities of the Spanish Government and European Regional Development Fund (ERDF) through project AGL2017-86840-C2-1-R, as well as the *Fundación Séneca*. Alberto Garre is grateful to *Fundación Séneca* for awarding him a post-doctoral grant (Ref: 20900/PD/18). The authors wish to acknowledge Ms Carmen M. Ruiz Sáez for her participation in the initial steps of this research.

Tables

Table 1. Model parameters used as reference for the calculations

	δ_{ref}(min)	$T_{ref}(ºC)$	$k(ºC^{-1})$	$T_c(ºC)$	$p/n(-)$	$z(ºC)$	$T_{min}(ºC)$[a]	$T_{max}(ºC)$[b]
Escherichia coli	11.96	52.5	0.58	56.95	1	5.18	52.5	60
Bacillus coagulans	7.3	90	0.4	99.97	2.04	12.01	90	100
Salmonella Senftemberg	3.17	55	0.3	56.19	0.38	5.84	55	62.5

[a]Minimum treatment temperature.
[b]Maximum treatment temperature.

Figures

Figure 1.Illustration of the uniform experimental designs considered (A) “Uni 2”, (B) “Uni 3” and (C) “Uni 4”.

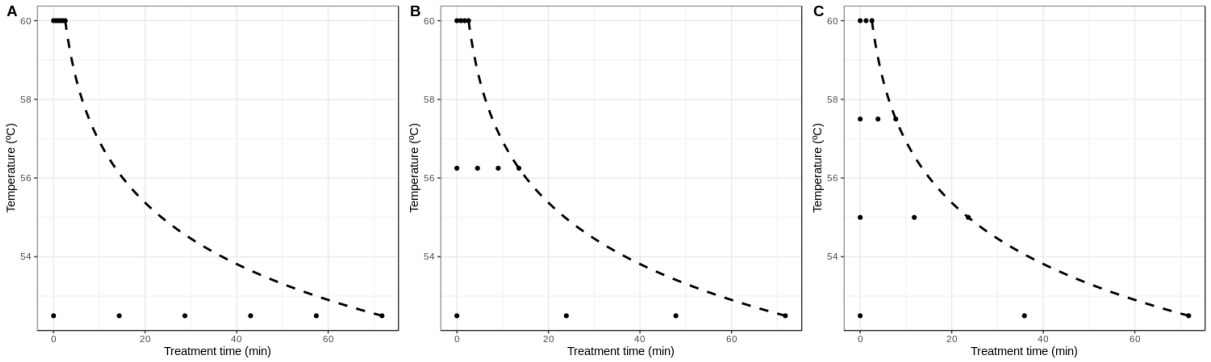

598

599 **Figure 2.**Local sensitivity functions and OEDs calculated (solid points) for (A) *B. coagulans*
600 and Bigelow model, (B) *B. coagulans* and Mafart model, (C) *B. coagulans* and Peleg model,
601 (D) *E. coli* and Bigelow model, (E)*E. coli* and Mafart model, (F)*E. coli* and Peleg model, (G)
602 *S.* Senftemberg and Bigelow model, (H) *S.* Senftemberg and Mafart model, (I) *S.* Senftemberg
603 and Peleg model.

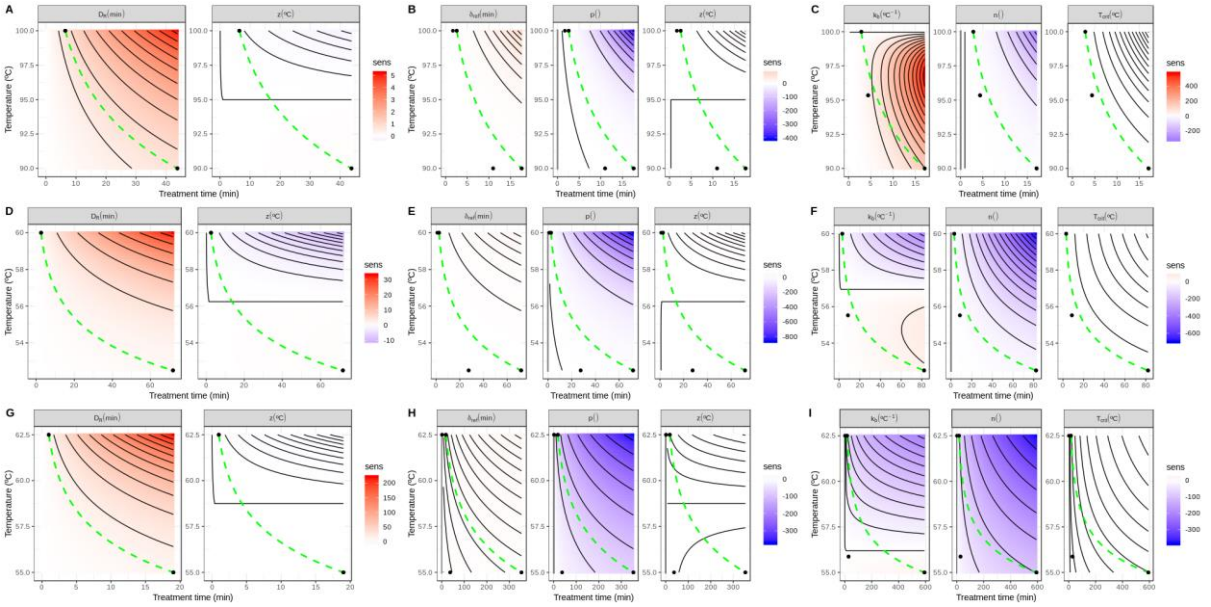

604

605 **Figure 3.** Boxplots of the relative standard deviation of parameters model in 1000 simulated
606 experiments for the D-value in the Bigelow model (A) and the δ-value in theMafart model (B)
607 when the T_{ref} is fixed to different values (see legend).

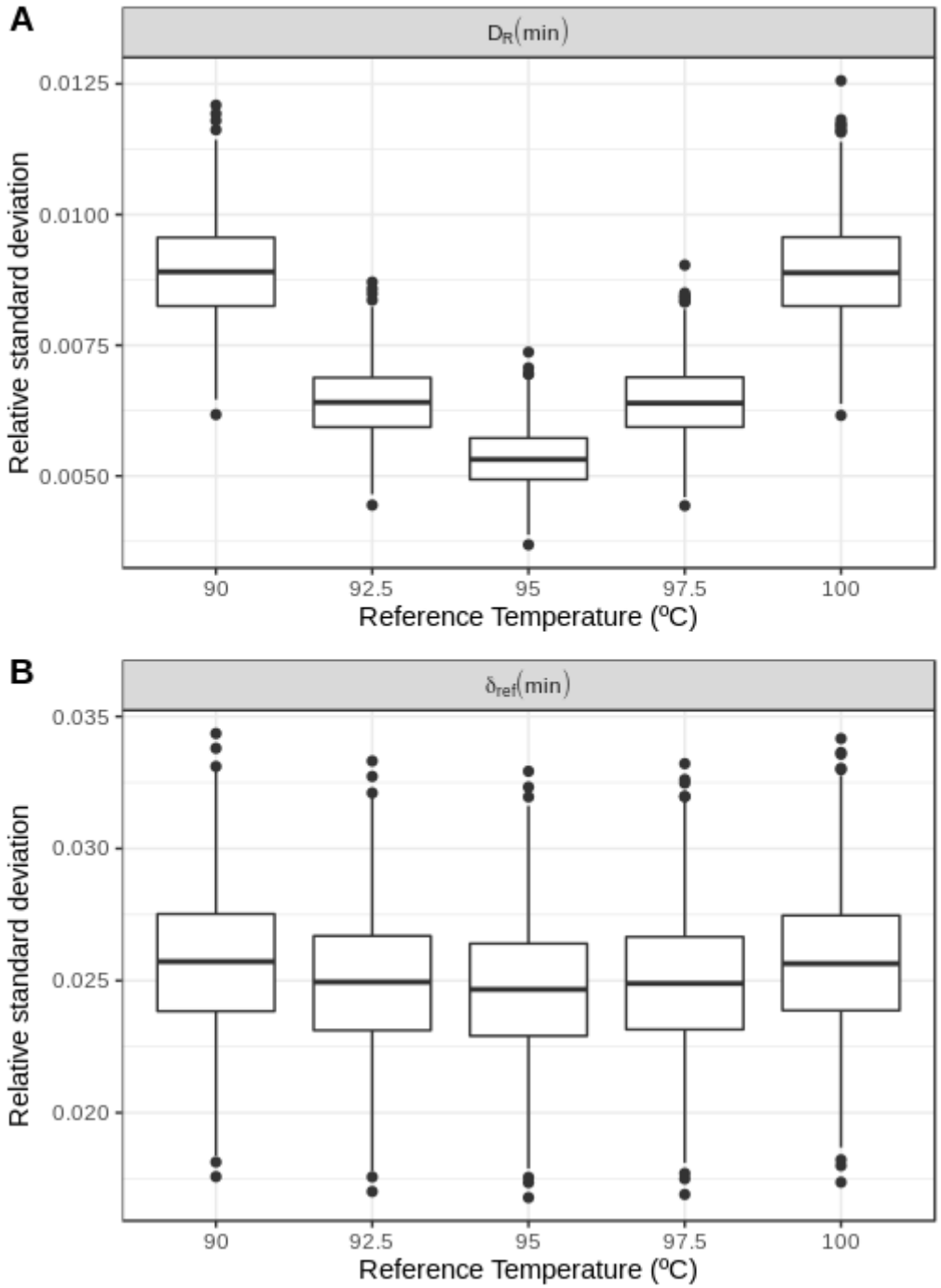

608

609 **Figure 4.**Inverse of the determinant of the *FIM* with respect to the number sampling points for
610 different experimental designs. (A) *B. coagulans* and Bigelow model, (B) *B. coagulans* and
611 Mafart model, (C) *B. coagulans* and Peleg model, (D) *E. Coli* and Bigelow model, (E) *E. coli*
612 and Mafart model, (F) *E. coli* and Peleg model, (G) *S.* Senftemberg and Bigelow model, (H) *S.*
613 Senftemberg and Mafart model, (I) *S.* Senftemberg and Peleg model and fixing the reference
614 temperature as the intermediate.

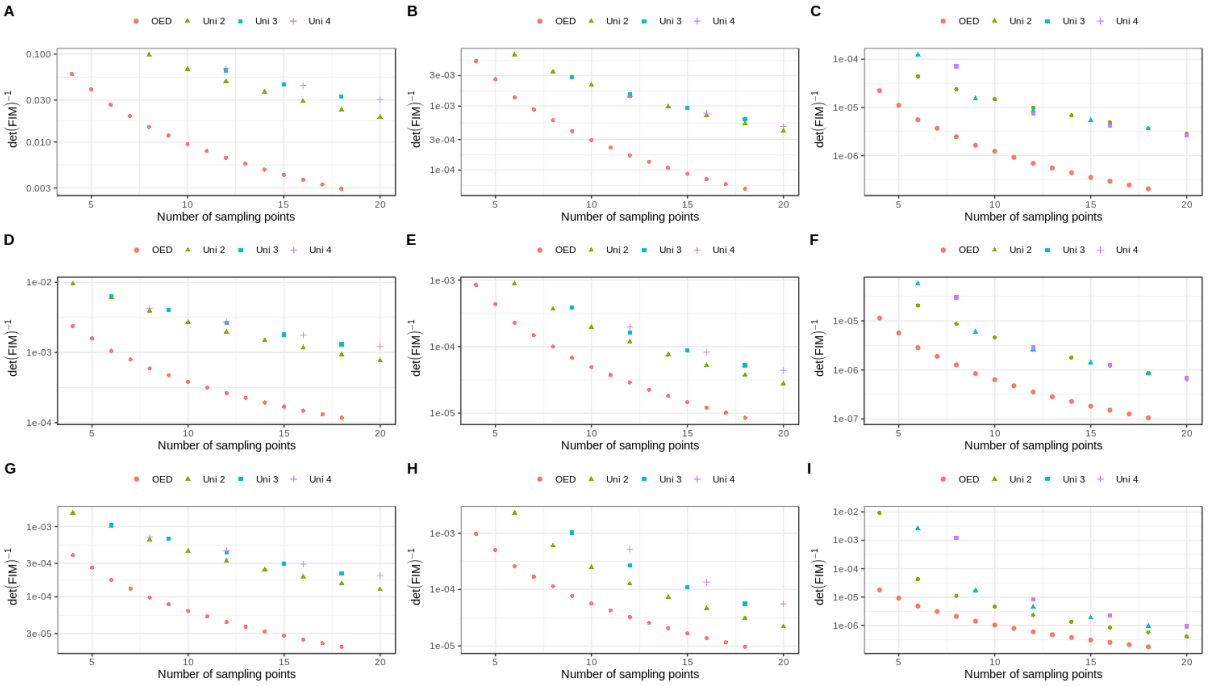

Figure 5. Boxplots of the relative standard deviations estimated in 100 simulated experiments with different experimental designs (OED and uniform). (A) *B. Coagulans* and Bigelow model, (B) *B. Coagulans* and Mafart model, (C) *B. Coagulans* and Peleg model, (D) *E. coli* and Bigelow model, (E) *E. coli* and Mafart model, (F) *E. coli* and Peleg model, (G) *S.* Senftemberg and Bigelow model, (H) *S.* Senftemberg and Mafart model, (I) *S.* Senftemberg and Peleg model and fixing the reference temperature as the intermediate.

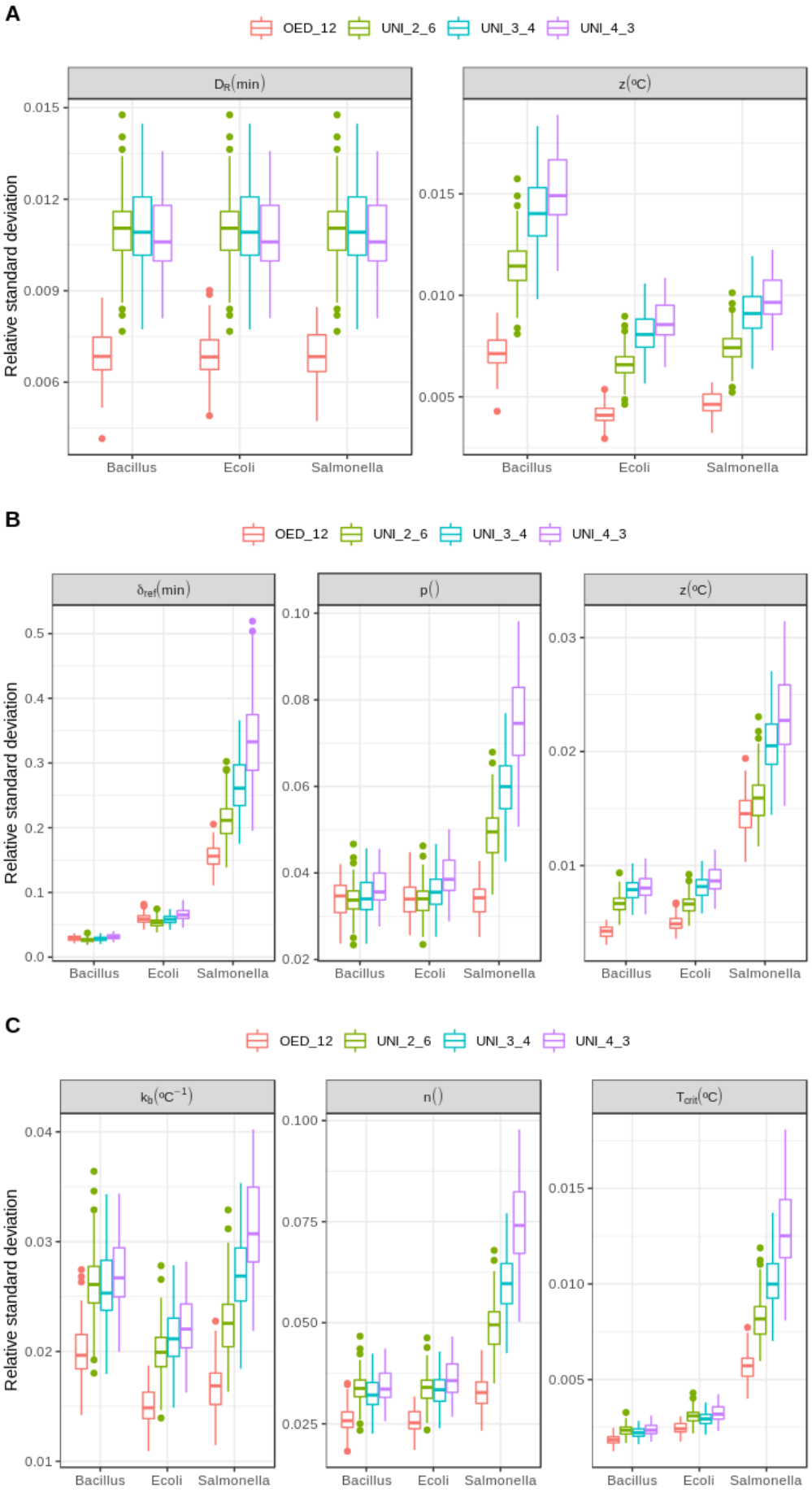
A
OED_12
UNI_2_6
UNI_3_4
UNI_4_3
$D_R(min)$
z(°C)
Relative standard deviation
Bacillus
Ecoli
Salmonella
B
$\delta_{ref}(min)$
p()
z(°C)
C
$k_b(°C^{-1})$
n()
$T_{crit}(°C)$

Supplementary Figure 1. Local sensitivity functions for the Mafart model with respect to parameters D_{ref}, z and p.(A)*B. coagulans*, $T_{ref} = T_{min}$, (B) *B. coagulans*, $T_{ref} = (T_{min} + T_{max})/2$, (C) *B. coagulans*, $T_{ref} = T_{max}$, (D) *E. coli*, $T_{ref} = T_{min}$, (E) *E. coli*, $T_{ref} = (T_{min} + T_{max})/2$, (F) *E. coli*, $T_{ref} = T_{max}$, (G) S. Senftemberg, $T_{ref} = T_{min}$, (H) S. Senftemberg, $T_{ref} = (T_{min} + T_{max})/2$, (I) S. Senftemberg, $T_{ref} = T_{max}$.

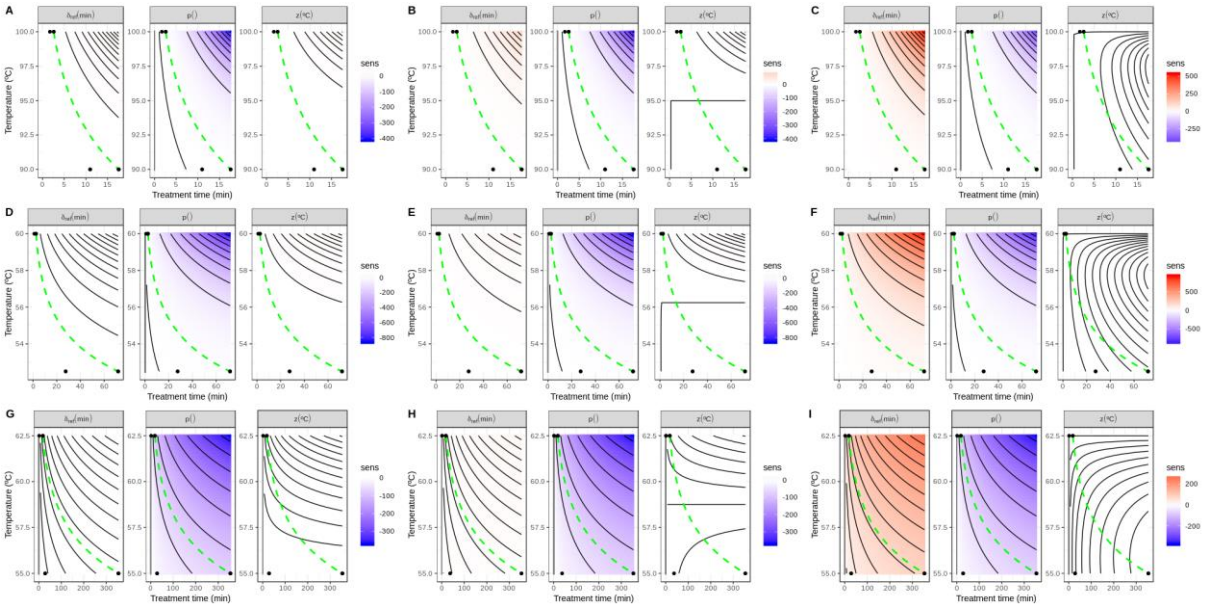

References

Asprey, S. P., & Macchietto, S. (2002). Designing robust optimal dynamic experiments. *Journal of Process Control*, *12*(4), 545–556. https://doi.org/10.1016/S0959-1524(01)00020-8

Balsa-Canto, E., Alonso, A. A., & Banga, J. R. (2008b). COMPUTING OPTIMAL DYNAMIC EXPERIMENTS FOR MODEL CALIBRATION IN PREDICTIVE MICROBIOLOGY. *Journal of Food Process Engineering*, *31*(2), 186–206. https://doi.org/10.1111/j.1745-4530.2007.00147.x

Balsa-Canto, Eva, Rodriguez-Fernandez, M., & Banga, J. R. (2007). Optimal design of dynamic experiments for improved estimation of kinetic parameters of thermal degradation. *Journal of Food Engineering*, *82*(2), 178–188.

Bigelow, W. D. (1921). The Logarithmic Nature of Thermal Death Time Curves. *The Journal of Infectious Diseases*, *29*(5), 528–536.

Box, G. E. P., Hunter, J. S., & Hunter, W. G. (2005). *Statistics for Experimenters: Design, Innovation, and Discovery*. Hoboken, N.J: Wiley-Blackwell.

Chik, A. H. S., Schmidt, P. J., & Emelko, M. B. (2018). Learning Something From Nothing: The Critical Importance of Rethinking Microbial Non-detects. *Frontiers in Microbiology*, *9*. https://doi.org/10.3389/fmicb.2018.02304

Cunha, L. M., Oliveira, F. A. R., Brandão, T. R. S., & Oliveira, J. C. (1997). Optimal experimental design for estimating the kinetic parameters of the Bigelow model. *Journal of Food Engineering*, *33*(1), 111–128. https://doi.org/10.1016/S0260-8774(97)00047-2

Datta, A. K. (1993). Error estimates for approximate kinetic parameters used in food literature. *Journal of Food Engineering*, *18*(2), 181–199. https://doi.org/10.1016/0260-8774(93)90035-I

de Aguiar, P. F., B. Bourguignon, Khots, M. S., Massart, D. L., & Phan-Than-Luu, R. (1995). D-optimal designs. *Chemometrics and Intelligent Laboratory Systems*, *30*(2), 199–210. https://doi.org/10.1016/0169-7439(94)00076-X

den Besten, H. M. W., Berendsen, E. M., Wells-Bennik, M. H. J., Straatsma, H., & Zwietering, M. H. (2017). Two complementary approaches to quantify variability in heat resistance of spores of Bacillus subtilis. *International Journal of Food Microbiology*, *253*, 48–53. https://doi.org/10.1016/j.ijfoodmicro.2017.04.014

den Besten, H. M. W., Wells-Bennik, M. H. J., & Zwietering, M. H. (2018). Natural Diversity in Heat Resistance of Bacteria and Bacterial Spores: Impact on Food Safety and Quality. *Annual Review of Food Science and Technology*, *9*(1), 383–410. https://doi.org/10.1146/annurev-food-030117-012808

Dolan, K. D., & Mishra, D. K. (2013). Parameter estimation in food science. *Annual Review of Food Science and Technology*, *4*(1), 401–422. https://doi.org/10.1146/annurev-food-022811-101247

Dolan, K. D., Valdramidis, V. P., & Mishra, D. K. (2013a). Parameter estimation for dynamic microbial inactivation: which model, which precision? *Food Control*, *29*(2), 401–408. https://doi.org/10.1016/j.foodcont.2012.05.042

Dolan, K. D., Valdramidis, V. P., & Mishra, D. K. (2013b). Parameter estimation for dynamic microbial inactivation: which model, which precision? *Food Control*, *29*(2), 401–408. https://doi.org/10.1016/j.foodcont.2012.05.042

Doyle, M. E., & Mazzotta, A. S. (2000). Review of Studies on the Thermal Resistance of Salmonellae. *Journal of Food Protection*, *63*(6), 779–795. https://doi.org/10.4315/0362-028X-63.6.779

Doyle, M. E., Mazzotta, A. S., Wang, T., Wiseman, D. W., & Scott, V. N. (2001). Heat Resistance of Listeria monocytogenes. *Journal of Food Protection*, *64*(3), 410–429. https://doi.org/10.4315/0362-028X-64.3.410

EFSA Scientific Committee, Benford, D., Halldorsson, T., Jeger, M. J., Knutsen, H. K., More, S., … Hardy, A. (2018). Guidance on Uncertainty Analysis in Scientific Assessments. *EFSA Journal*, *16*(1). https://doi.org/10.2903/j.efsa.2018.5123

Egea, J. A., Henriques, D., Cokelaer, T., Villaverde, A. F., MacNamara, A., Danciu, D.-P., … Saez-Rodriguez, J. (2014). MEIGO: an open-source software suite based on metaheuristics for global optimization in systems biology and bioinformatics. *BMC Bioinformatics*, *15*, 136. https://doi.org/10.1186/1471-2105-15-136

Egea, J. A., Martí, R., & Banga, J. R. (2010). An evolutionary method for complex-process optimization. *Computers & Operations Research*, *37*(2), 315–324. https://doi.org/10.1016/j.cor.2009.05.003

690 Fernández, A., Ocio, M. J., Fernández, P. S., Rodrigo, M., & Martinez, A. (1999). Application
691 of nonlinear regression analysis to the estimation of kinetic parameters for two
692 enterotoxigenic strains ofBacillus cereus spores. *Food Microbiology*, *16*(6), 607–613.
693 https://doi.org/10.1006/fmic.1999.0282
694 Frías, J. M., Oliveira, J. C., Cunha, L. M., & Oliveira, F. A. (1998). Application of D-optimal
695 design for determination of the influence of water content on the thermal degradation
696 kinetics of ascorbic acid at low water contents. *Journal of Food Engineering*, *38*(1), 69–
697 85. https://doi.org/10.1016/S0260-8774(98)00099-5
698 Garcés-Vega, F., & Marks, B. P. (2014). Use of Simulation Tools To Illustrate the Effect of
699 Data Management Practices for Low and Negative Plate Counts on the Estimated
700 Parameters of Microbial Reduction Models. *Journal of Food Protection*, *77*(8), 1372–
701 1379. https://doi.org/10.4315/0362-028X.JFP-13-462
702 García, M. R., Vilas, C., Herrera, J. R., Bernárdez, M., Balsa-Canto, E., & Alonso, A. A. (2015).
703 Quality and shelf-life prediction for retail fresh hake (Merluccius merluccius).
704 *International Journal of Food Microbiology*, *208*, 65–74.
705 https://doi.org/10.1016/j.ijfoodmicro.2015.05.012
706 Garre, A., Clemente-Carazo, M., Fernández, P. S., Lindqvist, R., & Egea, J. A. (2018).
707 Bioinactivation FE: A free web application for modelling isothermal and dynamic
708 microbial inactivation. *Food Research International*, *112*, 353–360.
709 https://doi.org/10.1016/j.foodres.2018.06.057
710 Garre, A., Egea, J. A., Esnoz, A., Palop, A., & Fernandez, P. S. (2019). Tail or artefact?
711 Illustration of the impact that uncertainty of the serial dilution and cell enumeration
712 methods has on microbial inactivation. *Food Research International*.
713 https://doi.org/10.1016/j.foodres.2019.01.059

714 Garre, A., Fernández, P. S., Lindqvist, R., & Egea, J. A. (2017). Bioinactivation: Software for
715 modelling dynamic microbial inactivation. *Food Research International*, *93*, 66–74.
716 https://doi.org/10.1016/j.foodres.2017.01.012
717 Garre, A., González-Tejedor, G., Peñalver-Soto, J. L., Fernández, P. S., & Egea, J. A. (2018).
718 Optimal characterization of thermal microbial inactivation simulating non-isothermal
719 processes. *Food Research International*, *107*, 267–274.
720 https://doi.org/10.1016/j.foodres.2018.02.040
721 Garre, A., Penalver, J. L., Fernandez, P. S., & Egea, J. A. (2017). *bioOED: Sensitivity Analysis*
722 *and Optimum Experiment Design for Microbial Inactivation*.
723 Garre, A., Peñalver-Soto, J. L., Esnoz, A., Iguaz, A., Fernandez, P. S., & Egea, J. A. (2019).
724 On the use of in-silico simulations to support experimental design: A case study in
725 microbial inactivation of foods. *PLOS ONE*, *14*(8).
726 https://doi.org/10.1371/journal.pone.0220683
727 González-Tejedor, G. A., Martínez-Hernández, G. B., Garre, A., Egea, J. A., Fernández, P. S.,
728 & Artés-Hernández, F. (2017). Quality Changes and Shelf-Life Prediction of a Fresh
729 Fruit and Vegetable Purple Smoothie. *Food and Bioprocess Technology*, 1–13.
730 https://doi.org/10.1007/s11947-017-1965-5
731 Haas, C. N., Rose, J. B., & Gerba, C. P. (2014). *Quantitative Microbial Risk Assessment*
732 (Edición: 2). Wiley.
733 Haberbeck, L. U., Dannenhauer, C., Salomão, B. D. C. M., & De Aragão, G. M. F. (2013).
734 Estimation of the Thermochemical Nonisothermal Inactivation Behavior of Bacillus
735 Coagulans Spores in Nutrient Broth with Oregano Essential Oil. *Journal of Food*
736 *Processing and Preservation*, *37*(5), 962–969. https://doi.org/10.1111/j.1745-
737 4549.2012.00745.x

738 Havelaar, A. H., van Rosse, F., Bucura, C., Toetenel, M. A., Haagsma, J. A., Kurowicka, D.,
739 … Braks, M. A. H. (2010). Prioritizing Emerging Zoonoses in The Netherlands. *PLoS*
740 *ONE*, *5*(11), e13965. https://doi.org/10.1371/journal.pone.0013965
741 Huertas, J.-P., Ros-Chumillas, M., Esteban, M.-D., Esnoz, A., & Palop, A. (2015).
742 Determination of Thermal Inactivation Kinetics by the Multipoint Method in a Pilot
743 Plant Tubular Heat Exchanger. *Food and Bioprocess Technology*, *8*(7), 1543–1551.
744 https://doi.org/10.1007/s11947-015-1525-9
745 Jarvis, B. (2008). *Statistical aspects of the microbiological examination of foods.* S.l.: Elsevier
746 Academic Press.
747 Longhi, D.A., Martins, W. F., da, S., Carciofi, B. A. M., de, A., & Laurindo, J. B. (2017).
748 Optimal experimental design for improving the estimation of growth parameters of
749 Lactobacillus viridescens from data under non-isothermal conditions. *International*
750 *Journal of Food Microbiology*, *240*, 57–62.
751 https://doi.org/10.1016/j.ijfoodmicro.2016.06.042
752 Longhi, Daniel Angelo, da Silva, N. B., Martins, W. F., Carciofi, B. A. M., de Aragão, G. M.
753 F., & Laurindo, J. B. (2018). Optimal experimental design to model spoilage bacteria
754 growth in vacuum-packaged ham. *Journal of Food Engineering*, *216*, 20–26.
755 https://doi.org/10.1016/j.jfoodeng.2017.07.031
756 Mafart, P., Couvert, O., Gaillard, S., & Leguerinel, I. (2002). On calculating sterility in thermal
757 preservation methods: application of the Weibull frequency distribution model.
758 *International Journal of Food Microbiology*, *72*(1–2), 107–113.
759 https://doi.org/10.1016/S0168-1605(01)00624-9
760 McMeekin, T. A., Mellefont, L. A., & Ross, T. (2007). Predictive microbiology: past, present
761 and future. In *Modelling Microorganisms in Food* (pp. 7–21).
762 https://doi.org/10.1533/9781845692940.1.7

763 Nishii, R. (1993). Optimality of experimental designs. *Discrete Mathematics*, *116*(1), 209 –
764 225. http://dx.doi.org/10.1016/0012-365X(93)90402-F
765 Paquet-Durand, O., Zettel, V., & Hitzmann, B. (2015). Optimal experimental design for
766 parameter estimation of the Peleg model. *Chemometrics and Intelligent Laboratory*
767 *Systems*, *140*, 36–42. https://doi.org/10.1016/j.chemolab.2014.10.006
768 Peleg, M., & Cole, M. B. (1998). Reinterpretation of Microbial Survival Curves. *Critical*
769 *Reviews in Food Science and Nutrition*, *38*(5), 353–380.
770 https://doi.org/10.1080/10408699891274246
771 Poschet, F., Geeraerd, A. H., Van Loey, A. M., Hendrickx, M. E., & Van Impe, J. F. (2005).
772 Assessing the optimal experiment setup for first order kinetic studies by Monte Carlo
773 analysis. *Food Control*, *16*(10), 873–882.
774 https://doi.org/10.1016/j.foodcont.2004.07.009
775 Possas, A., Valdramidis, V., García-Gimeno, R. M., & Pérez-Rodríguez, F. (2019). High
776 hydrostatic pressure processing of sliced fermented sausages: A quantitative exposure
777 assessment for Listeria monocytogenes. *Innovative Food Science & Emerging*
778 *Technologies*, *52*, 406–419. https://doi.org/10.1016/j.ifset.2019.01.017
779 Ros-Chumillas, M., Garre, A., Maté, J., Palop, A., & Periago, P. M. (2017). Nanoemulsified D-
780 Limonene Reduces the Heat Resistance of Salmonella Senftenberg over 50 Times.
781 *Nanomaterials*, *7*(3), 65. https://doi.org/10.3390/nano7030065
782 Schenkendorf, R., Xie, X., Rehbein, M., Scholl, S., & Krewer, U. (2018). The Impact of Global
783 Sensitivities and Design Measures in Model-Based Optimal Experimental Design.
784 *Processes*, *6*(4), 27. https://doi.org/10.3390/pr6040027
785 Stamati, I., Akkermans, S., Logist, F., Noriega, E., & Van Impe, J. (2016). Optimal
786 experimental design for discriminating between microbial growth models as function of

suboptimal temperature: From in silico to in vivo. *Food Research International*, *89*, 689–700. https://doi.org/10.1016/j.foodres.2016.08.001

Thompson, K. M. (2002). Variability and Uncertainty Meet Risk Management and Risk Communication. *Risk Analysis*, *22*(3), 647–654. https://doi.org/10.1111/0272-4332.00044

van Asselt, E. D., & Zwietering, M. H. (2006). A systematic approach to determine global thermal inactivation parameters for various food pathogens. *International Journal of Food Microbiology*, *107*(1), 73–82. https://doi.org/10.1016/j.ijfoodmicro.2005.08.014

van Derlinden, E., Balsa-Canto, & Van Impe. (2010). (Optimal) experiment design for microbial inactivation. In *Advances in Food Safety and Food Microbiology*. *Progress on quantitative approaches of thermal food processing - Valdramidis, V.P. & Van Impe, J.F.M. (Eds)* (pp. 67–98). Retrieved from https://www.novapublishers.com/catalog/product_info.php?products_id=29798

Vilas, C., Arias-Mendez, A., Garcia, M. R., Alonso, A. A., & Balsa-Canto, E. (2018). Toward predictive food process models: A protocol for parameter estimation. *Critical Reviews in Food Science and Nutrition*, *58*(3), 436–449. https://doi.org/10.1080/10408398.2016.1186591

Villaverde, A. F. (2019). Observability and Structural Identifiability of Nonlinear Biological Systems. *Complexity*, *2019*, 1–12. https://doi.org/10.1155/2019/8497093

Villaverde, A. F., Barreiro, A., & Papachristodoulou, A. (2016). Structural identifiability of dynamic systems biology models. *PLOS Computational Biology*, *12*(10), e1005153.

Villaverde, A. F., Evans, N. D., Chappell, M. J., & Banga, J. R. (2019). Input-Dependent Structural Identifiability of Nonlinear Systems. *IEEE Control Systems Letters*, *3*(2), 272–277. https://doi.org/10.1109/LCSYS.2018.2868608